Transport and electrically detected electron spin resonance of microcrystalline silicon before and after electron irradiation

W. Bronner and M. Mehring*
2. Physikalisches Institut, Universität Stuttgart, D-70550 Stuttgart, Germany

R. Brüggemann†
Fachbereich Physik, Carl von Ossietzky Universität Oldenburg, D-26111 Oldenburg, Germany
(Received 15 November 2001; published 8 April 2002)

We have applied electro-optical techniques and electrically detected magnetic resonance to investigate microcrystalline silicon before and after irradiation with 1-MeV electrons. Irradiation with electrons induces pronounced changes in the optical and electronic properties, namely, an increase in subgap absorption as measured by the constant photocurrent method and a deterioration of the dark and photoconductive properties. Electrically detected magnetic resonance (EDMR) measured in the photocurrent mode shows an increased dangling-bond contribution and a change in the recombination path with sample irradiation. This is also reflected in the temperature-dependent Rose factor. Below 50 K we find an EDMR signal that we attribute to the recombination of conduction electrons in shallow traps with dangling bonds. We also find an ''enhancement'' EDMR signal in the dark current with a typical g value for dangling bonds and which is almost unaffected by electron irradiation.

DOI: 10.1103/PhysRevB.65.165212 PACS number(s): 72.20.Jv, 61.82.Fk, 76.30.−v

I. INTRODUCTION

Since the first report on microcrystalline silicon by Veprek and Mareček[1] in 1968 it has been established in the last few years as a promising thin-film material for a variety of optoelectronic applications like solar cells or thin-film transistors.[2,3] This heterogeneous material is also very interesting from a fundamental physical point of view allowing us to study optoelectronic properties and electronic transport in the transition from amorphous to crystalline solid state. Microcrystalline silicon consists of crystalline silicon nanometer sized grains, which often form columns growing perpendicular to the substrate surface. Around these columns are nanoscale disordered boundaries that can be considered as an amorphous phase. Two main low-temperature deposition techniques ($\leqslant 300\,^{\circ}$C) for microcrystalline silicon are plasma-enhanced chemical-vapor deposition (PECVD) (Refs. 4–7) with very high frequency and thermocatalytic or hot-wire CVD (HWCVD).[8,9]

Concerning the properties of PECVD microcrystalline-silicon solar cells, the effect of proton irradiation was studied as a test for the environmental conditions in space.[10] An electron-spin-resonance study on electron irradiated microcrystalline silicon from PECVD was performed by Malten *et al.*[11] In this paper we report on irradiation of microcrystalline silicon from HWCVD with 1-MeV electrons, partly to provide not only information for space applications but also for investigating the fundamental properties of microcrystalline silicon. Electronic transport in microcrystalline silicon is affected by carrier trapping and recombination via defects. Therefore, defects such as dangling bonds (DB) are efficiency-reducing objects with respect to solar cell applications. Electron irradiation is a method to create defects and to increase defect densities. Also, high-energy electrons generate defects within the crystalline silicon phases (which are expected to have low DB defect densities for as-deposited samples as discussed in the literature[7]) and not only on grain or column boundaries. In order to widen the experimental basis we have applied different experimental methods such as constant photocurrent method (CPM), steady-state photoconductivity (SSPC), dark conductivity, and electrically detected magnetic resonance (EDMR). Comparison of results from these different techniques allows us to draw firm and representative conclusions about the change in sample properties due to electron irradiation and defect creation.

II. EXPERIMENT

A. Sample details

The effect of electron bombardment on microcrystalline silicon from HWCVD was studied in a sample deposited with 5% silane in hydrogen at 300 °C with a thickness of 2 μm and on Corning 7059 glass as a substrate. The selected sample showed columnar structure and high crystalline volume fraction typical for highly crystalline microcrystalline silicon. More details on the deposition and general properties, including Raman spectra for estimation of the crystalline volume fraction, of the investigated HWCVD microcrystalline silicon can be found elsewhere.[12] The evaporated Al contacts, typically 1–2 cm wide with a gap of 0.5–2 mm, showed Ohmic characteristics. Electron irradiation was performed at 140 K with 1-MeV electrons with a dose of 2.7×10^{18} cm^{-2}, equivalent to a flux of 3.5×10^{13} cm^{-2} s^{-1} for about 21 h.

B. Experimental techniques

All different experimental methods have been carried out before and after electron bombardment. The photocurrent I_{ph} was measured under steady illumination with a red-light Helium-Neon (He:Ne) laser. We applied CPM[13] for the determination of low absorption coefficients α and the opto-

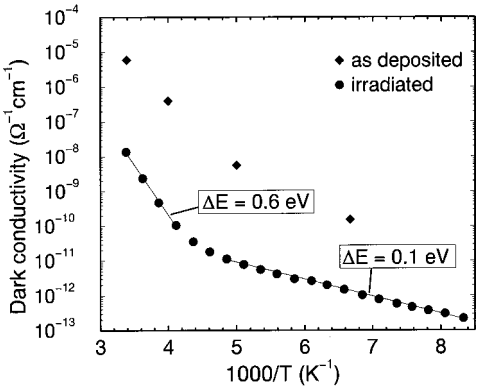

FIG. 1. Dark conductivity before and after electron bombardment of the microcrystalline sample.

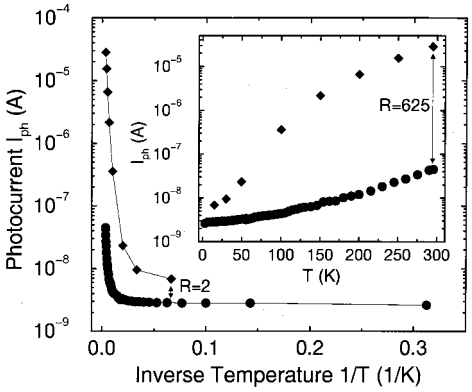

FIG. 2. Photocurrent before and after irradiation, measured at the same voltage and illumination conditions. The factor *R* reflects the reduction of the photocurrent due to the electron irradiation.

electronic spectroscopy of defect states. EDMR[14,15] measurements were performed in order to obtain microscopic information about charge-carrier transport. In all EDMR experiments microwave frequencies of about 9.5 GHz were applied in standard electron-spin-resonance spectrometers. For EDMR the current through the sample was measured while sweeping the magnetic field. For sample illumination, a He:Ne laser was used. The EDMR signal was lock-in detected with a magnetic-field modulation (having an amplitude of 0.5 mT, modulation frequency of 44 Hz, and microwave power of 200 mW).

III. RESULTS

Figure 1 shows the temperature dependence of the dark conductivity σ_d before and after electron bombardment. The room temperature σ_d drops by more than one order of magnitude upon irradiation. It shows thermally activated behavior with different activation energies ΔE. The activation energy and prefactor σ_0 for the as-deposited sample was determined from the high-temperature data as $\Delta E = 0.44$ eV and $\sigma_0 = 92$ S/cm. The values for the irradiated sample for ΔE are 0.1 eV for 120 K$<T<$210 K and 0.57 eV for 240 K$<T<$296 K. The conductivity prefactor σ_0 is orders of magnitude different for the two regimes and equals 65 S/cm for $\Delta E = 0.10$ eV and 2.3×10^{-9} S/cm for $\Delta E = 0.57$ eV. Analysis in terms of the $T^{1/4}$ law for variable-range hopping in three dimensions[16] also results in a straight line in an appropriate graphical representation for the low-T data. We derive a defect density at the Fermi level of 2×10^{18} cm^{-3} eV^{-1} assuming a localization length of 10 Å.

The photocurrent $I_{\rm ph}$ from 3 K to room temperature under high photon flux of 2×10^{17} cm^{-2} s^{-1}, as displayed in Fig. 2, deteriorates drastically upon irradiation, which is most pronounced at room temperature. At room temperature we observe a ratio $R = I_{\rm after}/I_{\rm before}$ of the photocurrent before and after the bombardment of $R = 625$. We note that this R value increases by about a factor of ten at a photon flux of only 10^{15} cm^{-2} s^{-1}. With decreasing temperature R decreases and reaches its lowest value of only about 2 at the lowest measured temperature of 7 K. The sample has an almost constant photocurrent for $T<40$ K, which rises drastically when increasing the temperature above 40 K.

We also determined the so-called Rose factor[17] γ, defined by $I_{\rm ph} \propto \phi^{\gamma}$ where ϕ is the photon flux of the sample illumination, from the intensity-dependent photocurrent. In a semiconductor with a single exponential band tail with an energy-independent tail parameter kT_0, the value for γ can be expressed as $\gamma = kT_0/(kT_0 + kT)$. An assumption in the Rose model is that the trapped charge in the band tail balances the charge from the recombination centers.

At low T, γ equals unity according to Fig. 3. The turnover to $\gamma<1$ behavior starts at higher temperatures for the irradiated sample. The decrease in γ is less pronounced and does not reach the value of 0.5 even for the highest measured temperature. Determining kT_0, for example, from measurements at 200 K, we find it to be 24 meV for the as-deposited sample and 328 meV for the irradiated sample.

Figure 4 shows the calibrated absorption coefficient α for different photon energies for the as-deposited sample and after irradiation as measured by CPM. For energies less than the band-gap energy of about 1.1 eV, α increases by one order of magnitude in the irradiated sample.

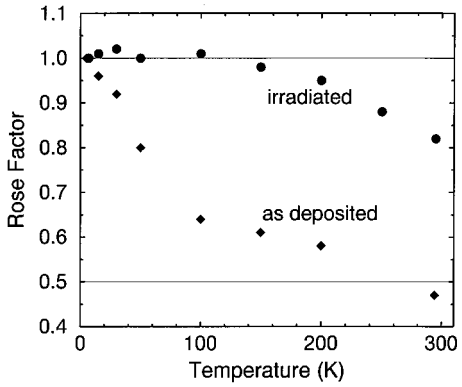

FIG. 3. Rose factor for the as-deposited and the irradiated samples.

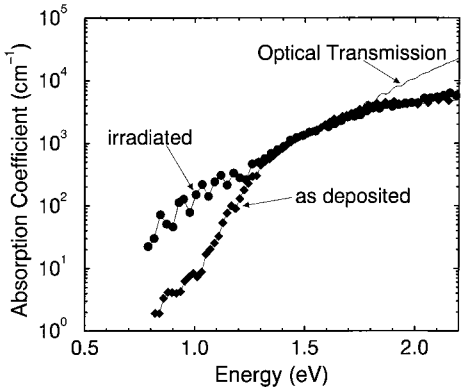

FIG. 4. Constant photocurrent method signal for the as-deposited sample and the irradiated sample calibrated with the absorption coefficient from optical measurements.

We could not detect any conventional electron-spin-resonance signal from the as-deposited sample. Considering the spectrometer detection limit, we estimated the upper value for the DB spin density as $N_d < 1 \times 10^{16}$ cm^{-3}. These measurements were restricted to the as-deposited sample because electron irradiation also creates defects in the glass substrate, making a proper analysis impossible.

To gain more information about changes in the transport mechanism, we studied EDMR before and after irradiation. Figure 5 displays the derivative EDMR signals for the as-deposited sample with amplitudes scaled to the same height in the temperature range from $T=7$ K to $T=200$ K. The signals were measured in the photocurrent mode. In the high-temperature range $T>100$ K one observes a single *quenching line*, i.e., a decrease in I_{ph} while sweeping the magnetic field through the resonance. The signature of the derivative EDMR signal allows us to distinguish between enhancement

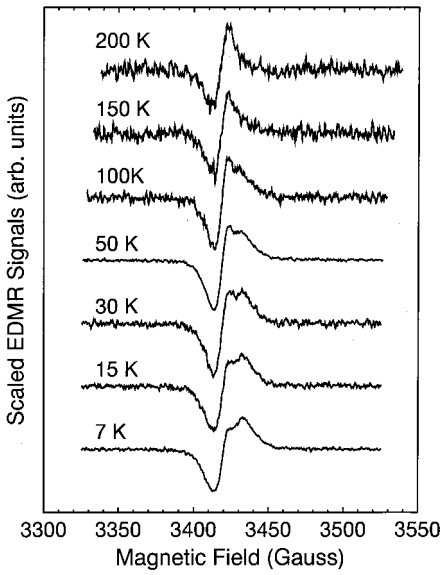

FIG. 5. Derivative EDMR spectra for the as-deposited sample for different temperatures. The signals were measured under illumination.

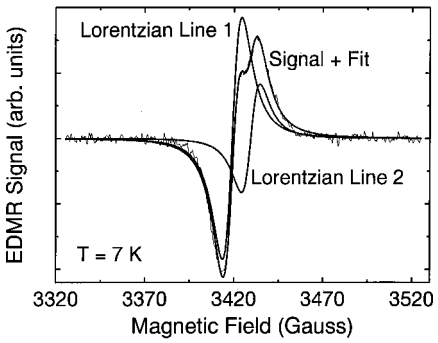

FIG. 6. Fitting of the EDMR spectra (measured at 7 K) with two Lorentzian lines.

and quenching lines. In the low-temperature range from 7 K to 100 K the sample still shows the dominant line but with an additional structure on the high-field side. This structure decreases with increasing temperature. The spectra in the low-temperature range could be well fitted by a superposition of a dominant Lorentzian line with a small Lorentzian line shifted to higher magnetic-field values $[g=1.9980(5)]$, which is illustrated in Fig. 6. This fitting procedure reveals a temperature-dependent g value for the dominant line with g $(T=7\ \text{K})=2.0040(5)$ and g $(T=200\ \text{K})=2.0050(5)$.

No additional signals appear after irradiation of the sample (see Fig. 7). The small feature at the high-field side is less pronounced for the irradiated sample and almost disappeared at 50 K.

We used the simulation (fit with two Lorentzian lines) to determine the temperature dependence of the signal height for the DBs and the conduction-electron (CE) contributions. Figure 8 shows the T dependence of the EDMR signal strength S for both contributions. $S(B)=\Delta\sigma/\sigma$ represents the relative change in conductivity $\Delta\sigma$ under microwave ir-

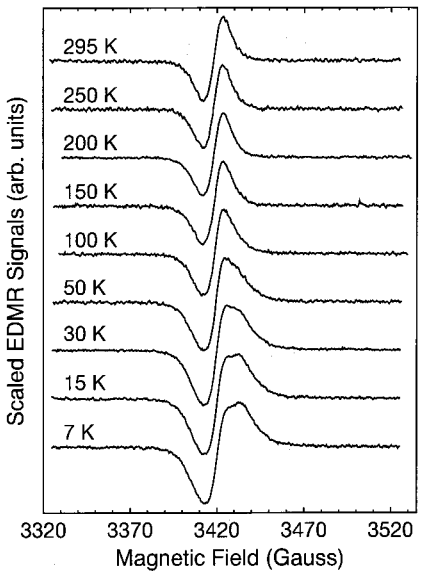

FIG. 7. Derivative EDMR spectra for the irradiated sample for different temperatures. The signals were measured under illumination.

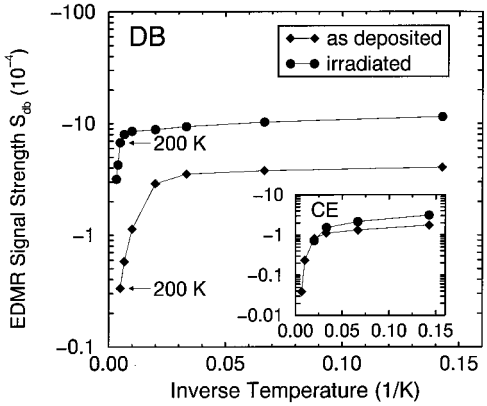

FIG. 8. EDMR signal strength for CE and DB contributions before and after electron bombardment.

radiation with varying magnetic field *B*. *S* is calculated at the resonance condition ($B=B_0$) by dividing the change of the photocurrent ΔI by I_{ph}. S_{DB} increases by a factor $F=S_{\mathrm{DBbefore}}/S_{\mathrm{DBafter}}$ of about 3 at 7 K and 20 at 200 K due to the sample irradiation. The change in *S* after irradiation for the CE line is within the measurement errors. The CE-line signal strength strongly decreases with increasing *T* until it disappears above 150 K. Also remarkable is the much weaker temperature dependence of S_{DB} for the irradiated sample for $T<200$ K.

EDMR measurements of the dark current showed a single enhancement signal (rising dark current at the resonance position) at room temperature before and after sample irradiation. For the as-deposited sample this signal could be also detected at lower temperatures down to 200 K. The dark signal has a *g* value of 2.0052(5). The room-temperature values for the signal strength are 1.9×10^{-5} before irradiation and 1.1×10^{-5} after irradiation.

IV. DISCUSSION

The increased value of α for energies less than the band-gap energy is determined by optical transitions that involve states in the band gap and delocalized states in the bands.[18] This is the evidence for an increase in the number of defect states in the band gap of microcrystalline silicon due to electron bombardment. The higher number of defect states is expected to also influence the transport characteristics and the recombination behavior of the charge carriers.

This high defect density induces a changeover in the dark-conductivity transport from extended states at higher *T* to hopping through defect states at low *T* in the irradiated sample. The low σ_0 value in the low-*T* region for the irradiated sample in Fig. 1 is incompatible with conduction in extended states. A defect density of a few times of 10^{18} $\mathrm{cm}^{-3}\,\mathrm{eV}^{-1}$ as deduced from Mott's law can well be responsible for the transport via hopping in this temperature range. The values for σ_0, calculated from the data at higher *T* and for the as-deposited sample can be related to conduction in extended states and are comparable to values found in the literature[19,20] where, according to the Meyer-Neldel rule, σ_0 varies with the activation energy.

The drop in the dark conductivity at higher *T* after irradiation can be understood in terms of a change of the Fermi level with the increase in the density of gap states. In a Si:H the density of negatively charged DBs balances that of positive DBs and determines the Fermi-level position. A similar behavior can be anticipated here. The Fermi level will shift if the newly created states after irradiation require a change in the charge balance.

The drop of the photocurrent after electron irradiation also reflects the increased number of recombination states in the band gap. The *T*-dependent photoconductivity shows the typical behavior observed for microcrystalline silicon,[21–23] which is indicated by the almost constant I_{ph} for $T<40$ K. Illustrated by the low *R* in this temperature region, we find nearly no change in the low-*T* photocurrent after irradiation, which can be consistently explained by the energy-loss hopping behavior that is unaffected by electron bombardment and does not depend on the defect density. In amorphous or microcrystalline silicon at low temperature, photogenerated carriers lose energy by thermalizing into deeper localized states, or finally by recombination. The photocurrent for temperatures typically below 50 K arises from energy-loss hopping of carriers, which means that the carriers hop to states of lower energy. It is limited by the duration for the thermalization process resulting in $\gamma\approx1$.

On the other hand, there is a strong change after irradiation in the progression of I_{ph} and γ for $T>40$ K. After irradiation the monomolecular recombination behavior dominates over the whole temperature range. Consequently, we suggest that the main recombination path is the recombination of excited electrons with irradiation induced defects in the band gap.

Analysis of the *T*-dependent γ values according to the simple Rose model with a single exponential tail does not lead to the same value of kT_0 at different temperatures. We suggest that the density of states has a more complicated distribution in the vicinity of the quasi-Fermi energy $E_{fn}(T)$, which shifts with *T*, and cannot be described by the same kT_0 at the different $E_{fn}(T)$, respectively. What we can say is that the irradiated sample has a much broader distribution, varying less in energy than in the as-deposited sample. As already mentioned, kT_0 equals 24 meV for the as-deposited sample and 328 meV for the irradiated sample from measurements at 200 K.

The EDMR signals before and after irradiation show a dominant line with an additional line contribution at low temperatures. No additional signals appear after irradiation. The EDMR *g* values of the dominant line are close to the previously observed values of $g=2.0043$ and $g=2.0052$. The latter one was attributed to the DBs.[24–27] The resonance at $g=2.0043$ cannot be unambiguously identified. Most obvious is the assignment to DB states in a different environment.[28] We suggest that the signal of the dominant line in the detected EDMR signal consists of a weighted average of two lines that cannot be resolved. This, however, does not affect our analysis concerning the consequence of the irradiation.

Due to the *g* value of 1.998(5) for the small Lorentzian line that contributes to the lineshape at low temperatures, the

line can be assigned to CE's in shallow traps.[23,29] The CE line decreases in amplitude with increasing temperature (see Fig. 8). A strong increase of the linewidth[28] and a temperature-dependent recombination path could be the origin for this.

At low temperatures recombination takes place via conduction electrons in tail states or in the conduction band with DBs.[23,29] Electron bombardment does not influence this behavior, but it does increase the signal amplitudes of the DB signal contribution. In the standard spin-pair model three main dynamic rates such as the spin-relaxation rate T_S^{-1}, dissociation rate k_D or the singlet-recombination rate k_S define the value of the EDMR signal strength S for constant density of recombination centers.[30] In the saturation limit one obtains

$$S=\frac{\Delta\sigma}{\sigma}\approx-\frac{1}{2}\frac{k_D k_S}{(4k_D+k_S)(k_D+T_S^{-1})}. \tag{1}$$

In microcrystalline silicon k_S is much larger than k_D.[31] This simplifies Eq. (1) to

$$\frac{\Delta\sigma}{\sigma}\approx-\frac{1}{2}\frac{k_D}{k_D+T_S^{-1}}. \tag{2}$$

In terms of spin-pair dynamics a decrease in k_D and an increase in T_S^{-1} would result in a reduced EDMR signal strength as is observed in Fig. 8 with increasing temperature. Both the as-deposited and the irradiated samples show basically the same temperature-dependent behavior. This is most likely due to an increase in the relaxation rate with increasing temperature.

It is expected that electron irradiation can at most increase the relaxation rate and not reduce it. The observed enhancement of the EDMR signal for the irradiated sample can not therefore, be attributed to a relaxation effect. Also an increase in k_D due to irradiation is very unlikely, because the distance between electron and DB should be reduced. Instead, we conclude that the larger DB density provides more recombination centers in the irradiated samples resulting in an enhanced EDMR signal.

Another interesting observation is the increase in the ratio F with increasing temperature and the almost constant S_{DB} for the irradiated sample. We suggest that the reason for these effects is the different recombination behavior for the as-deposited and the irradiated samples at higher temperatures, due to the charge balance requirement. Both samples show recombination of excited electrons with DBs at low temperatures. With increasing temperature, however, the as-deposited sample shows a deviation from monomolecular behavior while S_{DB} and γ decrease. The irradiated sample still shows monomolecular recombination with almost constant S_{DB} and $\gamma\approx1$ below $T<200$ K. Here, the charge balance is mainly determined by the high density of dangling bonds whereas in the as-deposited sample shallow-trapped charge (perhaps in the band tails) plays the role of adjusting the charge neutrality, leading to the gradual change in γ with increasing T.

Finally, we discuss the dark-current EDMR signals. In microcrystalline silicon, these signals are assigned to spin-dependent hopping between the DB defect states. They were only detected in samples with high defect densities.[32,33] It was also shown that the EDMR signal strength rises with increasing defect density. This is in contrast to what we see in our sample. Although the defect density for the as-deposited sample was lower than 1×10^{16} cm^{-3}, we could detect such a dark-current EDMR signal. More surprisingly though, the EDMR signal strength did not increase after electron irradiation. Therefore, the origin of the dark EDMR signal in our sample is not clear yet and needs further investigations.

V. CONCLUSION

We investigated microcrystalline silicon from HWCVD before and after irradiation with 1-MeV electrons by SSPC, dark conductivity, CPM, and EDMR. After electron irradiation σ_d drops by more than two orders of magnitude due to the change of the Fermi energy as a consequence of the increase of the density of gap states. I_{ph} is also lowered after irradiation because of the larger number of recombination states in the gap. This drop is reflected by a factor R between 625 and 6000 in the photon-flux range at room temperature and by a factor $R=2$ at 15 K. The low-T results can be reconciled with energy-loss hopping behavior that is not affected by the large increase in the density of gap states due to electron irradiation. The gap states could be identified as DBs by EDMR. No other defect not yet known in microcrystalline silicon could be detected. The different temperature dependence of the Rose factor γ and of the EDMR signal strength S_{DB} before and after irradiation indicates a change in the recombination path. The irradiated sample shows primarily monomolecular recombination of excited electrons with DBs. The observation of the EDMR signal at low temperatures can be understood as recombination of CEs in shallow traps with DBs. The creation of dangling bonds and the deteriorating influence of electron irradiation on the electronic properties of microcrystalline silicon needs to be considered for applications. The experiments reported here show that one must take the change in the optical and degradation of transport properties due to high-energy particles in this material into account when considering it for future space applications.

ACKNOWLEDGMENTS

The authors thank J. Guillet and J. E. Bourée, Ecole Polytechnique, Palaiseau for sample deposition and A. Jasenek, Institut für Physikalische Elektronik, Universität Stuttgart for the electron irradiation performed at the Institut für Strahlenphysik, Universität Stuttgart. We are grateful to M.B. Schubert for the access to the CPM setup at the Institut für Physikalische Elektronik. R.B. thanks the Deutsche Forschungsgemeinschaft, Bonn, Germany, for financial support.

*Electronic address: m.mehring@physik.uni-stuttgart.de
†Electronic address: rudi.brueggemann@uni-oldenburg.de

[1] S. Vepřek and V. Mareček, Solid-State Electron. **11**, 683 (1968).
[2] J. Meier, R. Flückiger, H. Keppner, and A. Shah, Appl. Phys. Lett. **65**, 860 (1994).
[3] R.E.I. Schropp, K.F. Feenstra, E.C. Molenbroek, H. Meiling, and J.K. Rath, Philos. Mag. B **76**, 309 (1997).
[4] S. Oda, J. Noda, and M. Matsumura, Jpn. J. Appl. Phys., Part 1 **29**, 1889 (1990).
[5] G. Willeke, in *Amorphous and Microcrystalline Semiconductor Devices Physics*, edited by J. Kanicki (Artech House, Boston, 1992), Vol. 2, p. 55.
[6] R. Flückiger, J. Meier, H. Keppner, M. Götz, and A. Shah, in *Conference Record 23rd IEEE Photovoltaic Specialists Conference, Louisville, 1993* (IEEE, New York, 1993) p. 839.
[7] F. Finger, J. Müller, C. Malten, and H. Wagner, Philos. Mag. B **77**, 805 (1998).
[8] H. Matsumura, Jpn. J. Appl. Phys., Part 2 **25**, L949 (1986).
[9] H. Wanka, M. B. Schubert, A. Hierzenberger, and V. Baumung, in *Proceedings of the 14th European Photovoltaic and Solar Energy Conference, Barcelona, 1997*, edited by H. A. Ossenbrink *et al.* (Stephens, Bedford, UK, 1997), p. 1005.
[10] J. Kuendig, M. Goetz, J. Meier, P. Torres, L. Feitknecht, P. Pernet, X. Niquille, A. Shah, L. Gerlach, and E. Fernandez, in *Proceedings of the 16th European Photovoltaic and Solar Energy Conference, Glasgow, 2000*, edited by H. Scheerer, B. McNelis, W. Palz, H. A. Ossenbrink, and P. Helm (James & James, London, 2000), p. 986.
[11] C. Malten, F. Finger, P. Hapke, T. Kulessa, C. Walker, R. Carius, R. Flückiger, and H. Wagner, in *Microcrystalline and Nanocrystalline Semiconductors*, edited by L. Prus, M. Hiyase, B.W. Collins, F. Koch, and C.C. Tsai, Mater. Res. Soc. Symp. Proc. **358** (Materials Research Society, Pittsburgh, 1995), p. 757.
[12] R. Brüggemann, J.P. Kleider, C. Longeaud, D. Mencaraglia, J. Guillet, J.E. Bourée, and C. Niikura, J. Non-Cryst. Solids **266-269**, 258 (2000).
[13] J. Vanecek, J. Kocka, J. Stuchlik, and A. Triska, Solid State Commun. **39**, 1199 (1981).
[14] M. Stutzmann, M.S. Brandt, and M.W. Bayerl, J. Non-Cryst. Solids **266-269**, 1 (2000).
[15] A. Maier, A. Grupp, and M. Mehring, Solid State Commun. **99**, 623 (1996).
[16] For example, N. F. Mott and E. A. Davies, *Electronic Processes in Noncrystalline Solids*, 2nd ed. (Oxford University Press, Oxford, UK, 1979).
[17] A. Rose, *Concepts in Photoconductivity and Allied Problems* (Wiley, New York, 1963).
[18] W. Jackson, N.M. Johnson, and D.K. Biegelsen, Appl. Phys. Lett. **43**, 195 (1983).
[19] R. Brüggemann, M. Rojahn, and M. Rösch, Phys. Status Solidi A **166**, R11 (1998).
[20] J. Kočka, J. Stuchlik, Ha Stuchlikova, V. Svrcek, P. Fojtik, T. Mates, K. Luterova, and A. Fejfar, Appl. Phys. Lett. **79**, 2540 (2001).
[21] J.H. Zhou, S.D. Baranovskii, S. Yamasaki, K. Ikuta, K. Tanaka, M. Kondo, A. Matsuda, and P. Thomas, Phys. Status Solidi B **205**, 147 (1998).
[22] R. Brüggemann and W. Bronner, Phys. Status Solidi B **212**, R15 (1999).
[23] W. Fuhs, P. Kanschat, and W. Fuhs, J. Vac. Sci. Technol. B **18**, 1792 (2000).
[24] S. Vepřek, Z. Ibqual, R.O. Kühne, P. Capezzuto, F.-A. Sarott, and J.K. Gimzewski, J. Phys. C **16**, 6241 (1983).
[25] F. Finger, C. Malten, P. Hapke, R. Carius, R. Flückiger, and H. Wagner, Philos. Mag. Lett. **70**, 247 (1994).
[26] T. Ehara, Appl. Surf. Sci. **113/114**, 126 (1997).
[27] M. Kondo, T. Nishimiya, K. Saito, and A. Matsuda, J. Non-Cryst. Solids **227-230**, 1031 (1998).
[28] J. Müller, F. Finger, R. Carius, and H. Wagner, Phys. Rev. B **60**, 11 666 (1999).
[29] P. Kanschat, K. Lips, and W. Fuhs, J. Non-Cryst. Solids **266-269**, 524 (2000).
[30] T. Eickelkamp, S. Roth, and M. Mehring, Mol. Phys. **95**, 967 (1998).
[31] C. Böhme and K. Lips, Appl. Phys. Lett. **79**, 4363 (2001).
[32] D. Will, C. Lerner, W. Fuhs, and K. Lips, in *Amorphous and Microcrystalline Silicon Technology, edited by S. Wagner, M. Hack, E.A. Schiff, R. Schropp, and I. Shimizu, Mater. Res. Soc. Symp. Proc.* **467** (Materials Research Society, Pittsburgh, 1997), p. 361.
[33] K. Lips, P. Kanschat, D. Will, C. Lerner, and W. Fuhs, J. Non-Cryst. Solids **227-230**, 1021 (1998).